



POWER ENGINEERING, AUTOMATION, AND ENERGY PERFORMANCE

Research article

<https://doi.org/10.17073/2500-0632-2022-1-57-65>**Automatic control system for walking dragline excavator digging**L. D. Pevzner  , N. A. Kiselev

Russian Technological University MIREA, Moscow, Russian Federation

 lpevzner@msmu.ru**Abstract**

This paper presents the results of the development of automatic control systems for walking dragline excavator digging process. The process enables operational productivity to be enhanced through optimizing digging process. This also prevents extreme loads on machinery and hoist cable deflection. The paper also describes mathematical models of the electric drives of the main excavator machinery which form the bucket motion and the model of cable length change. Further the study will analyse the structure of the control system and the automatic digging algorithm. Computer modeling findings are also described to confirm the operability of the automatic digging algorithm. Computer simulation of the processes in electric drives of main machinery of a walking dragline in digging operations was performed by means of SimInTech software. The automatic control system optimizes digging trajectory with very fast penetration with permissible overregulation following digging at a constant cut depth. The integrated system of dragline operation process control is practically independent due to the following factors: the automatic digging control system in combination with automatic systems for transporting the loaded bucket to dump and the empty bucket to the face; the automatic main machinery overload protection systems; and the system of control over safe bucket movement in the dragline working space

Keywords

mining machinery, walking dragline excavator, bucket, operation, digging, mathematical models, automation, electric drive, algorithm, control, controller

For citation

Pevzner L. D., Kiselev N. A. Automatic control system for walking dragline excavator digging. *Mining Science and Technology (Russia)*. 2022;7(1):57–65. <https://doi.org/10.17073/2500-0632-2022-1-57-65>

ЭНЕРГЕТИКА, АВТОМАТИЗАЦИЯ И ЭНЕРГОЭФФЕКТИВНОСТЬ

Научная статья

Система автоматического управления процессом черпания шагающего экскаватора-драглайнаЛ. Д. Певзнер  , Н. А. Киселев

Российский технологический университет – МИРЭА, г. Москва, Российская Федерация

 lpevzner@msmu.ru**Аннотация**

Актуальность исследований, результаты которых составляют основу систем автоматического управления рабочей операцией черпания шагающего экскаватора-драглайна, обусловлена необходимостью повышения производительности машины и снижением предельных нагрузок на механизмы и канатные системы. Анализу подвергается система автоматического управления рабочей операцией черпания шагающего экскаватора-драглайна, позволяющая обеспечить повышение его эксплуатационной производительности за счет приближения процесса черпания к рациональному.

На основе методов математического моделирования систем электропривода основных механизмов экскаватора-драглайна составлены имитационные математические модели, которые описывают движение ковша и канатных систем. Результаты компьютерного модельного исследования, выпол-

ненные программными средствами SimInTech, подтвердили работоспособность предложенного алгоритма автоматического черпания.

Разработанная система автоматического управления операцией черпания позволяет приблизить траекторию черпания к оптимальной, обеспечивая предельно быстрое заглубление с допустимым перерегулированием и последующим равномерным черпанием с постоянной толщиной срезаемой стружки. Показатели качества управляемого процесса черпания в породах с удельным сопротивлением $k_p = 1,45 \pm 0,45$ кг/см² и $k_p = 3,35 \pm 0,75$ кг/см² практически совпадают: перерегулирование в первом случае 7,2 %, во втором – 10,4 %, время регулирования в первом случае 4 с, во втором – 3,5 с.

Разработанная система автоматического управления операцией черпания вместе с автоматическими системами транспортирования груженого ковша в отвал и порожнего ковша в забой, системами автоматической защиты от перегрузки главных механизмов, системой контроля безопасного движения ковша в рабочем пространстве драглайна позволяют повысить уровень автоматизации экскаватора-драглайна и его производительность

Ключевые слова

горная машина, шагающий экскаватор-драглайн, ковш, операция, черпание, автоматизация, математические модели, электропривод, алгоритм, управление, регулятор

Для цитирования

Pevzner L. D., Kiselev N. A. Automatic control system for walking dragline excavator digging. *Mining Science and Technology (Russia)*. 2022;7(1):57–65. <https://doi.org/10.17073/2500-0632-2022-1-57-65>

Introduction

A walking dragline excavator is a highly effective mining machine with great technological capabilities. It is widely used in the mining industry for stripping via a non-transport process flow sheet applicable in open-cut mining of such minerals as: coal; shale; ores of ferrous and nonferrous metals; gold; and raw materials for chemical industry [1, 2].

The experience of operating these machines at coal mines in Russia over a long period shows that walking dragline efficiency does not exceed 70 %.

High efficiency of walking dragline excavator operation can be ensured by automating the following control processes: main working operations for transporting loaded buckets to the dump and empty bucket to the face; automation of digging process, through automatic limitation of dynamic loads in electromechanical systems; and providing safe control of excavation process [3–5].

Research aimed at the development of automatic control systems for walking dragline excavator digging process is relevant, since such systems will allow operational productivity to be enhanced through optimizing digging process, thus avoiding extreme loads on machinery and hoist cable deflection.

1. Mathematical model of digging operation

Mathematical modeling of walking dragline excavator processes is a first and important stage to resolving the question of creating algorithms and control systems for the individual devices/units and the machine as a whole [6, 7].

In order to compile a mathematical model of digging, it was assumed that drag cables are weightless and non-extensible, and that the rate of change in their

length is constant. In the process of rock mass digging using a dragline excavator bucket, a resistance force F_c , arises. This can be represented as a sum of three forces F_1, F_2, F_3 – a bucket friction force on soil; cutting resistance force; and resistance force to movement of the rock mass dozing capacity. The bucket friction force on soil is defined by the expression $F_1 = \beta N$, where β – is the bucket friction on soil coefficient, and N is the normal support response. Cutting resistance force is determined by the expression $F_2 = k_p B_b h$, where k_p – specific resistance of rock mass to cutting, B_b – width of bucket, h – bucket depth of cut.

Figure 1 shows bucket and forces applied to it.

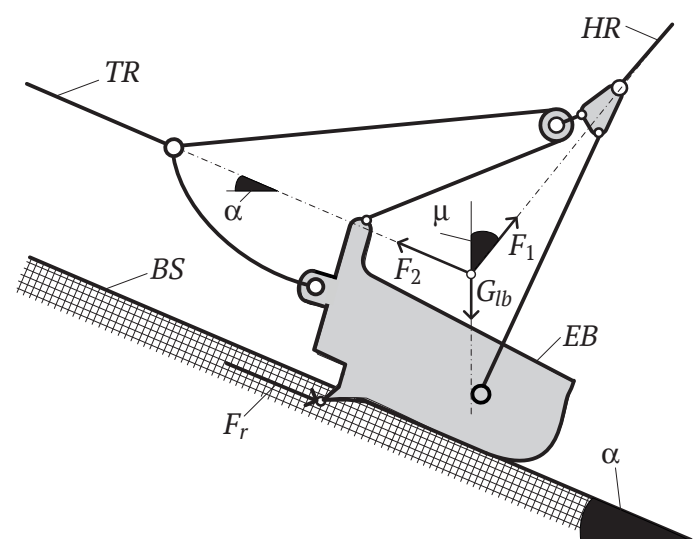


Fig. 1. Diagram of forces applied to the bucket: HR – hoist cables; TR – drag cables; BS – face surface; EB – excavator bucket; F_r – digging resistance forces; F_1 – tension of hoist cables; F_2 – tension of drag cables; G_{lb} – weight of loaded bucket; α – angle of face slope; μ – deviation of drag cables from vertical direction

The diagram of forces applied to the bucket (Fig. 1) was used for further calculation. This was used to derive the equations of bucket movement dynamics in the axes of hoist and drag cables length $\{l_1, l_2\}$.

$$\begin{aligned} m_{lb}(t)\ddot{l}_1(t) &= F_1(t) - G_{lb}(t)\cos\mu - (F_2(t) + F_r(t))\sin(\alpha - \mu), \\ m_{lb}(t)\ddot{l}_2(t) &= F_2(t) - G_{lb}(t)\sin\alpha - (F_1(t) + F_r(t))\sin(\alpha - \mu), \end{aligned} \quad (1)$$

where $m_{lb}(t)$ is the mass of the bucket together with the contained rock mass.

2. Mathematical model of electric drives of hoisting and traction mechanisms

The electric drives of the hoisting and traction mechanisms of ESh 20.90 walking excavator have the same structure [8, 13]: generator – motor (G-M) with thyristor excitation; and control system according to the diagram of double-loop slave regulation with power circuit current controller and generator voltage controller.

The mathematical model¹ of the hoisting mechanism–bucket–traction mechanism system was developed

¹ Technical documentation for ESH 20.90. URL: https://maxi-exkavator.ru/exclopedia/technic/esh-2090_omz

in accordance with the flowchart shown in Fig. 2, under the conditions of known assumptions [9, 14].

A system of equations presents the electric drive mathematical model for any of the mechanisms of hoisting or traction, the input of which is $U_i(t)$ – voltage of the command device for setting speed of changing length of the corresponding cable, and the output $\omega(t)$ – is the motor shaft speed (2).

$$u_{VR}(t) = \text{sat}(U_i(t) - k_1 e(t); k_{VR}, u_{VR}^*),$$

$$u_{CR}(t) = \text{sat}\left(u_{VR}(t) - k_4 I(t) + k_5 \int_0^t (u_{VR}(t) - k_4 I(t)) dt; k_{CR}, u_{CR}^*\right),$$

$$u_{MA}(t) = k_{MA} u_{CR}(t),$$

$$T_{TC} \dot{u}_{TC}(t) + u_{TC}(t) = k_{TC}(t) u_{MA}(t), \quad (2)$$

$$T_G \dot{u}_G(t) + u_G(t) = k_G u_{TC}(t),$$

$$T_{AC} \dot{I}(t) + I(t) = k_{AC}(u_G(t) - C_E \omega(t)),$$

$$J \dot{\omega}(t) = C_M I(t) - M_R.$$

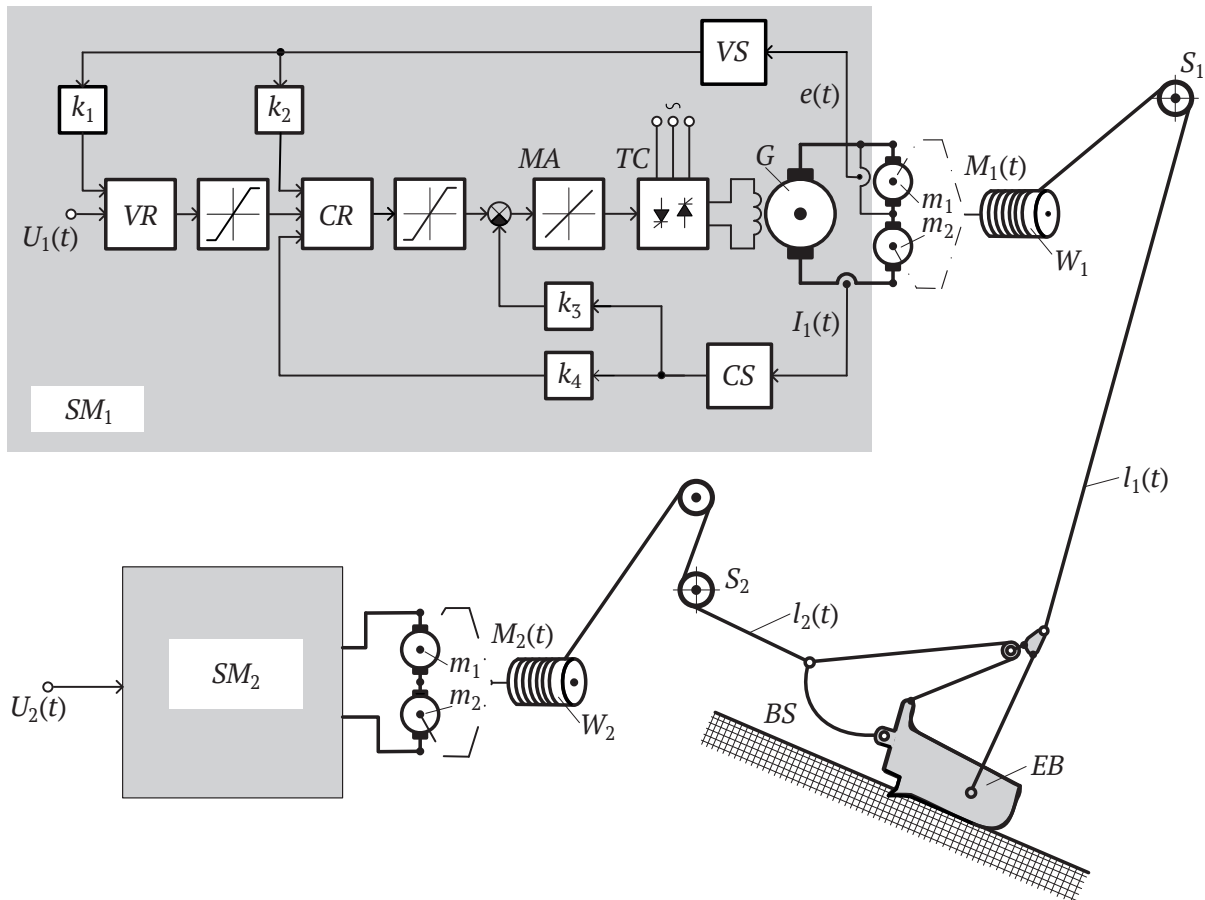


Fig. 2. Schematic diagram of the hoisting mechanism–bucket–traction mechanism system:

S_1 – fairlead sheaves; S_2 – pointing units; l_1 – hoist cables; l_2 – drag cables; EB – excavator bucket; BS – face surface; W_1 – hoisting mechanism winch; W_2 – traction mechanism winch; SM_1, SM_2 – power control system for hoisting and traction motors, respectively; CS – hoisting drive current sensor; VS – generator voltage sensor; VR – voltage controller; CR – current controller; MA – matching amplifier; TC – thyristor converter; k_1, k_2, k_3, k_4 – loop gain blocks; m_1, m_2 – motors; M_1, M_2 – driving torques of hoisting and traction, respectively; U_1, U_2 – hoisting and traction motions assignments, respectively



In these expressions:

$u_{VR}(t)$, $u_{CR}(t)$, $u_{MA}(t)$, $u_{TC}(t)$, $u_G(t)$ are the output signals of the voltage controller, current controller, matching amplifier, thyristor converter, and generator, respectively; u_{VR}^* , u_{CR}^* – threshold values of signals of voltage and current controllers; k_{VR} , k_{CR} – limiting controller transfer factors; T_{TC} , T_G , T_{AC} – response time of thyristor converter, generator, and armature circuit; k_1 , k_4 , k_5 – parameters of p-controller of voltage and PI-controller of current; k_{MA} , k_{TC} , k_G , k_{AC} – transfer factors of matching amplifier, thyristor converter, generator, and armature circuit; J – mass moment of inertia of mechanism, reduced to motor shaft; $I(t)$ – current of the motor armature circuits; C_E , C_M – design motor constants; M_R – resistance torque in drive, reduced to motor shaft.

We performed a synthesis procedure of the PI-controller for the inner circuit – current loop, by adjusting it to the modular optimum. The controller parameters and its transfer function

$$W_{CR}(s) = \frac{4.6s + 1}{6.69s}$$

were obtained using the ESh 20.90² excavator specifications.

The parameter of proportional (p) controller of voltage and its transfer function were defined according to the modular optimum synthesis procedure

$$W_{VR}(s) = 8.32.$$

² Some technical characteristics of walking dragline excavator ESh 20.90 used for obtaining transfer functions of its model driving media:

- transfer factor of thyristor excitation device $k_{TC} = 44,3V/V$;
- time response of thyristor excitation device $T_{TC} = 0,01s$;
- generator transfer factor $k_G = 14,0V/V$;
- generator time response $T_G = 4,6s$;
- motor armature circuit transfer factor $k_{AC} = 31,0\Omega^{-1}$;
- motor armature circuit time response $T_{AC} = 0,05s$;
- motor rotor and hoisting/traction system winch product of inertia reduced to motor shaft $J = 517Nm/A$;
- motor constructional constants $C_E = 8,64V/s$, $C_M = 8,64Nm/A$;
- current sensor transfer factor $k_{CS} = 0,0029V/A$;
- voltage sensor transfer factor $k_{VS} = 0,0081V/V$;
- thresholds of voltage and current controllers signals $10V$;
- stop motor armature current $I_{stop} = 3400A$;
- generator rated voltage $U_G^* = 1230V$; $U_{Gnom} = 1230V$;
- nominal motor rotational rate $\omega_M^* = 70,6s^{-1}$;
- transfer ratio of hoisting/traction mechanism reducing gear $r = 22,53$;
- performance coefficient of hoisting/traction mechanism reducing gear $\eta = 0,9$;
- hoisting/traction mechanism winch barrel radius $r_W = 0,9m$;
- electromechanical time response of motor $T_M = 0,06s$;
- weight of empty bucket $G_b = 220kN$;
- weight of loaded bucket (with rock mass) $G_{lb} = 480kN$.

Technical documentation for ESh 20.90 https://maxi-exkavator.ru/excapedia/technic/esh-2090_omz

3. Digging operation modeling

The model of bucket movement in interaction with the face consists of the following: the model of traction and hoisting electric drives (2); the model of bucket movement while digging (1); and technical data of ESh 20.90 dragline excavator. The model structure is shown in Fig. 3.

3.1. Model studies of processes in electric drives of main machinery

SimInTech software was selected for computer simulation of key machinery (mechanisms') drives for a walking dragline excavator in the course of digging operations.

The modeling of processes of changing lengths of hoist and drag cables and processes in electric drives was performed on the basis of model representations (1), (2). The schematic diagrams of the computer models of the hoisting and traction electric drives and cable lengths changes are presented in Figs. 4 and 5.

The model parameters are taken from the specifications [11] for ESh 20.90 walking dragline excavator. The hoisting and traction electric drives use GPE-2500–750UZ generator with a rated voltage of 1200 V and MPE-1000-630UZ motors with the rated angular velocity of $70.6 s^{-1}$.

Findings from the model studies shown in Fig. 6 show that the electric drive model run-up time amounted to 3 s. The steady-state rate of cable length change $v^{max} = 0.25 ms^{-1}$ agrees with oscillograms of real curves of dragline electric drives run-up and braking, as presented in [12].

The model studies confirm the adequacy of the description of dynamic processes in electric drives and the kinematics of drag and hoist cables motion.

3.2. Modeling of digging process

The model studies of the digging process were performed according to schematic diagram in Fig. 3. The digging process is performed with a constant traction speed equal to $1ms^{-1}$. The rational digging process is carried out either with maximum initial depth of cut or with a constant depth of cut.

In the first case, digging time is minimal, since maximum power of excavator traction and hoisting drives is used. However, this method can lead to locking of the traction drive and, just as importantly, to difficulties in subsequent digging due to the unevenness of the face profile.

In the second digging case, the face relief is processed evenly. The power of excavator drives is not used fully, the dynamic loads exclude the possibility of bucket locking.

The uniform bucket filling method was taken as a basis for the synthesis of the digging process control system, for which the adjustable value was the depth of cut.

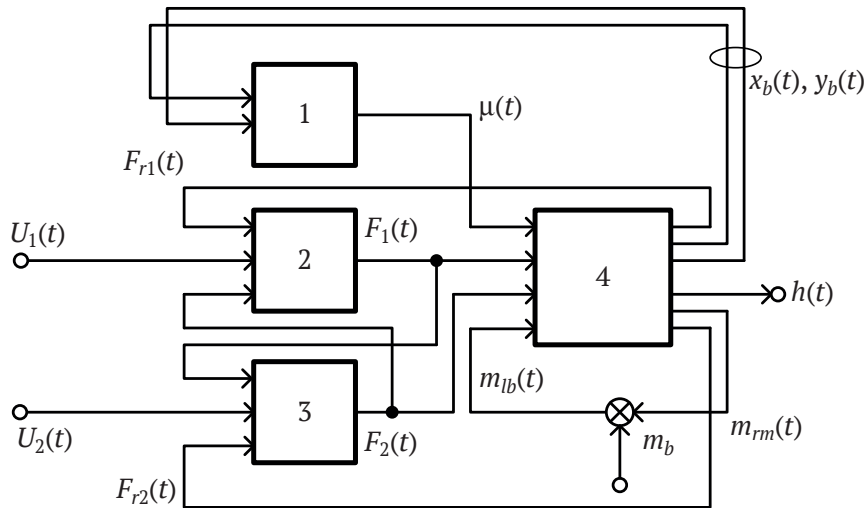


Fig. 3. The structure of model of bucket motion while digging:

block 1 – determination of angle μ ; block 2 – model of hoisting mechanism; block 3 – model of traction mechanism; block 4 – model of face; $U_1(t), U_2(t)$ – setting tensions of hoisting and traction drives; $x_b(t), y_b(t)$ – current Cartesian coordinates of bucket position; μ – angle between hoist cables and y-axis; $h(t)$ – value of bucket penetration into the face; $m_b, m_{rm}(t), m_{lb}(t)$ – mass of the empty bucket, rock mass in bucket, mass of loaded bucket, respectively; $F_1(t), F_2(t)$ – force acting on bucket from traction and hoisting mechanisms, respectively; $F_{r2}(t)$ – force acting on bucket from the face along the axis of drag cable, including friction force, rock cutting resistance, resistance to movement of rock dozing capacity; $F_{rN}(t)$ – force normally acting on bucket from, including gravity force and rock cutting resistance

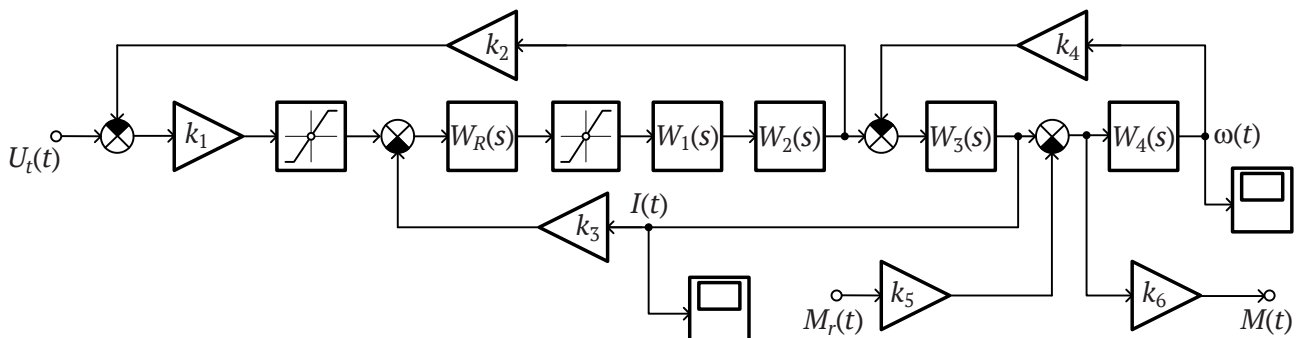


Fig. 4. Schematic diagram of electric drives model:

$U_t(t)$ – setting signal from master controller; coefficients: $k_1 = 0.324, k_2 = 0.0081, k_3 = 0.0029, k_4 = 17.28, k_5 = 0.00231, k_6 = 389.769$; transfer functions of link models: $W_1(s) = 44.3/(0.01s + 1), W_2(s) = 14.0/(4.6s + 1), W_3(s) = 31/(0.05s + 1), W_4(s) = 0.032/s$; $\omega(t)$ – motor shaft speed; $M_r(t)$ – drag torque to motor shaft; $M(t)$ – hoisting/traction winch shaft torque

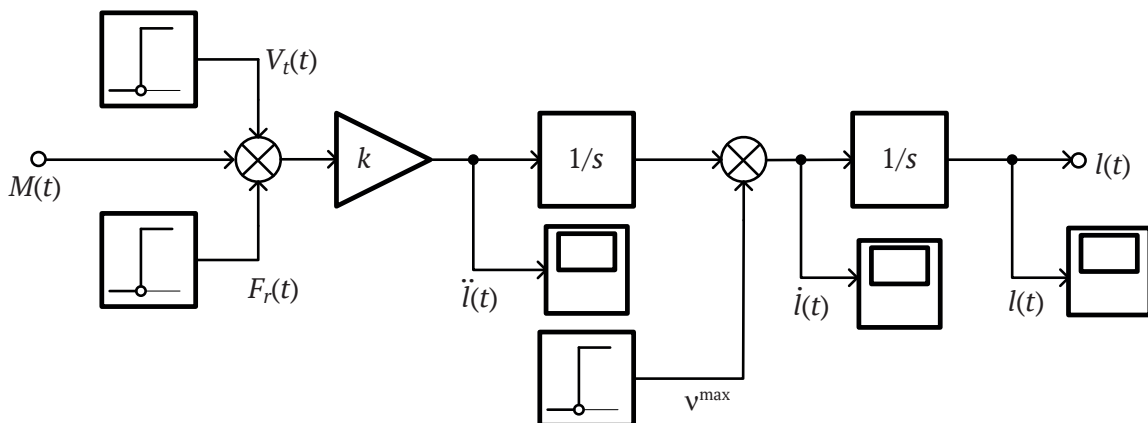


Fig. 5. Schematic diagram of the computer model of cable length change:

$V_r(t)$ – command signal for cable length change rate. For the maximum rate the command-apparatus signal is 10V; the maximum digging resistance force $\max F_r(t) = 201,858.7234 \text{ kH}$; $M(t)$ – hoisting/traction winch shaft torque; factor $k = 3.2987e^{-06}, v^{\max} = 0.2497 \text{ mc}^{-1}$ (maximum cable length change rate); $i(t), \dot{i}(t), l(t)$ – current values of acceleration, rate, and length of hoist/drag cables, respectively

The automatic control system structure for the digging process is presented in Fig. 7.

The system investigated the possibility of using a PID-controller with parameters adjusted using the Ziegler-Nichols method: $k_p = 46$, $k_i = 33.3$, $k_d = 15.19$. The setting of a small, 0.3 m, and significantly larger, 0.75 m depth of cuts was performed. The findings

of the study are shown in Fig. 8. In both cases, unacceptable overregulation and long regulation time took place.

The use of the integral controller allowed a considerable decrease in overregulation. However, at the same time, the transition process became considerably longer.

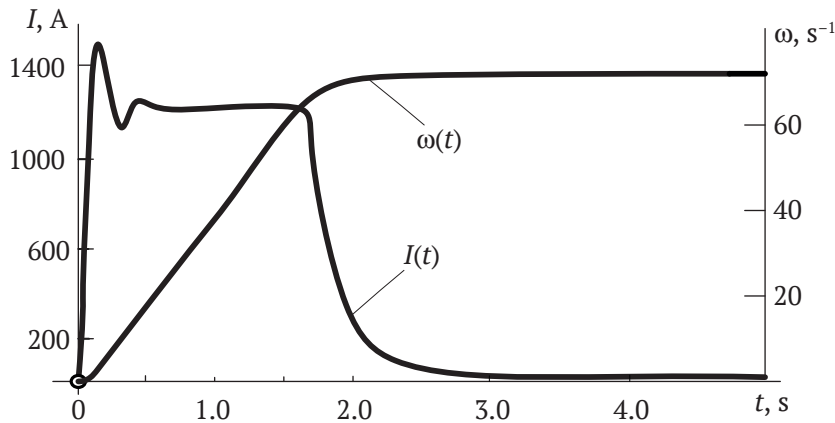


Fig. 6. Findings of simulation studies:
 I – starting up to speed current, A; ω – motor shaft speed, s^{-1}

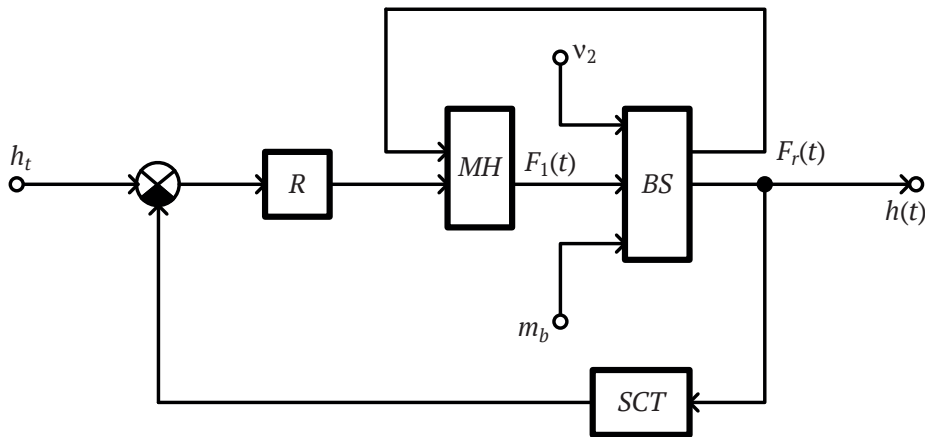


Fig. 7. Digging automatic control system structure:
 block R – controller; block MH – model of hoisting mechanism; block BS – face model; $h(t)$ – current depth of cut; $F_r(t)$ – current resistance to rock mass (soil) cutting; SCT – depth of cut sensor; h_t – assigned depth of cut

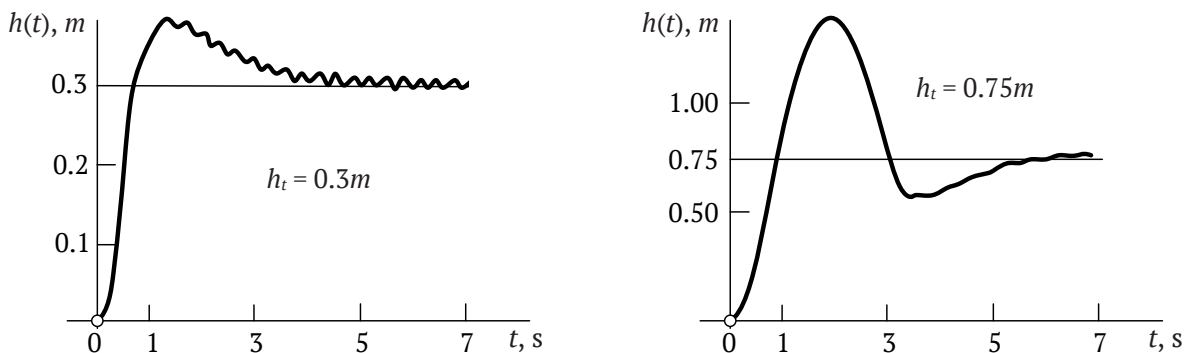


Fig. 8. Changing of cut depth at different parameters of three term controller (PID)

The studies showed inefficiency of linear controllers. Therefore, proceeding from the logic of real work of the operator, a two-step algorithm of forming control action on the traction drive is proposed.

The digging process is presented in two phases: digging, and movement of the bucket with constant cut depth. The second phase is provided by linear algorithm of three term controller, the first phase of digging is formed by non-linear algorithm

$$u(h; \mu) = \begin{cases} 0, & \varepsilon \leq h_0(\mu), \\ -10, & \varepsilon > h_0(\mu), \end{cases}$$

$$\varepsilon(t) = h_3 - h(t).$$

In the expression, $h_0(\mu)$ – is the braking path when the bucket penetrates into soil. This depends on the hoist cable tension force, or more precisely, on the angle of inclination of the hoist cables.

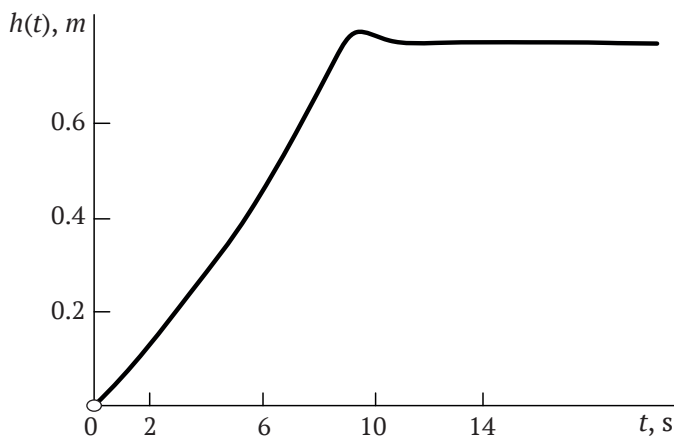


Fig. 9. Depth of cut changes with integral controller

The meaning of this algorithm is that the bucket's penetration into a rock (cutting) is performed with maximum force, and the movement should be terminated at the set depth. Thus, cut depth is a nonlinear function of time, while the rate of the depth of cut change is an almost linear function of time, as seen from Fig. 10.

Structural flowchart of automatic control system of walking dragline digging process is presented in Fig. 11.

Model research into the functionality of the digging process automatic control system process was carried out for the following case: weight of the empty bucket $m_b = 22,000$ kg; $\alpha = 30^\circ$; slope angle of the face; $v_0 = 1$ ms⁻¹ – drag cable speed when digging; $h_t = 0,85$ m – assigned cut depth at specific resistance to digging $k_p = 1.45 \pm 0.45$ kg/cm²; $h_t = 0.45$ m – assigned cut depth at specific resistance to digging $k_p = 3.35 \pm 0.75$ kg/cm².

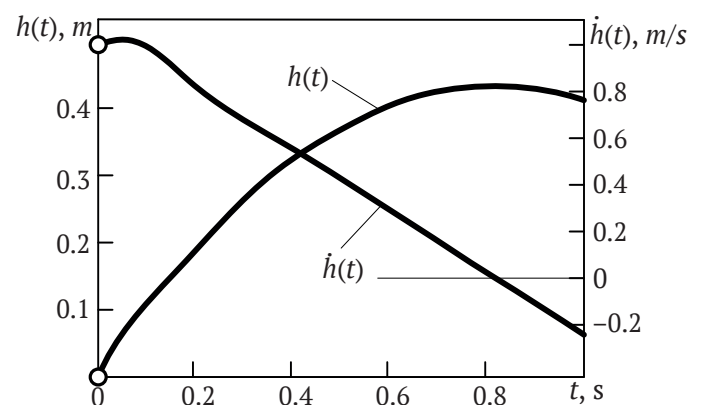


Fig. 10. Depth of cut change with non-linear controller: $h(t)$ – current cut depth; $\dot{h}(t)$ – rate of change in depth of cut

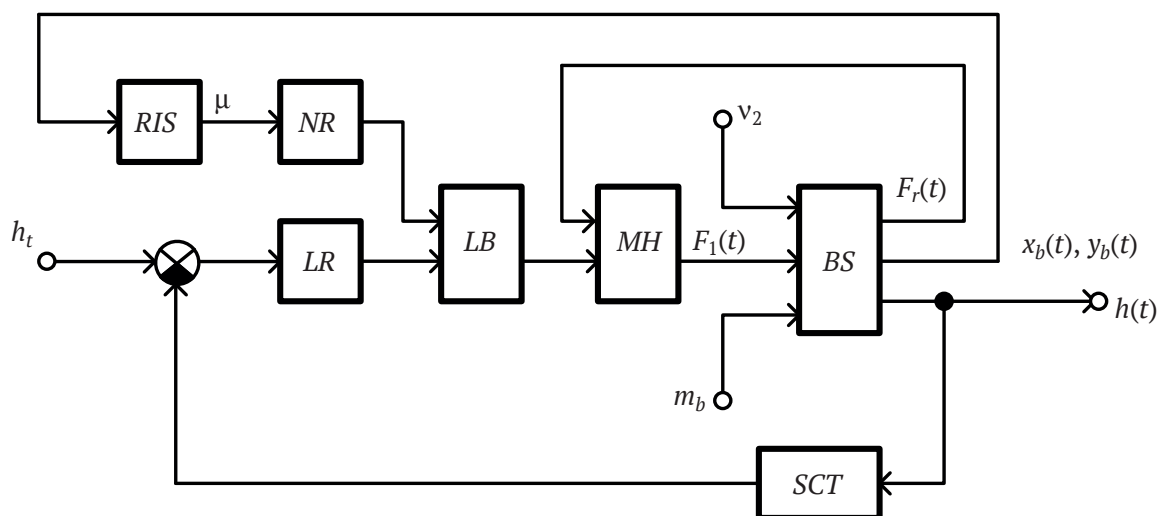


Fig. 11. Structural flowchart of automatic control system of walking dragline digging process: LR – linear controller; NR – non-linear controller; LB – logic block; RIS – hoist cables angle sensor; MH – hoisting mechanism model; BS – face model; SCT – depth of cut sensor; h_b – assigned depth of cut; $h(t)$ – current depth of cut; $x_b(t), y_b(t)$ – current Cartesian coordinates of bucket; block $F_r(t)$ – current resistance to rock mass cutting

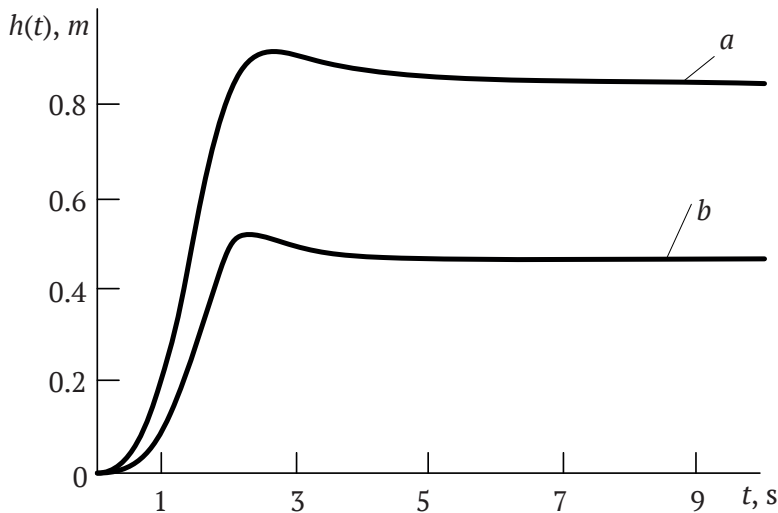


Fig. 12. Changing depth of cut in the process of automatic digging

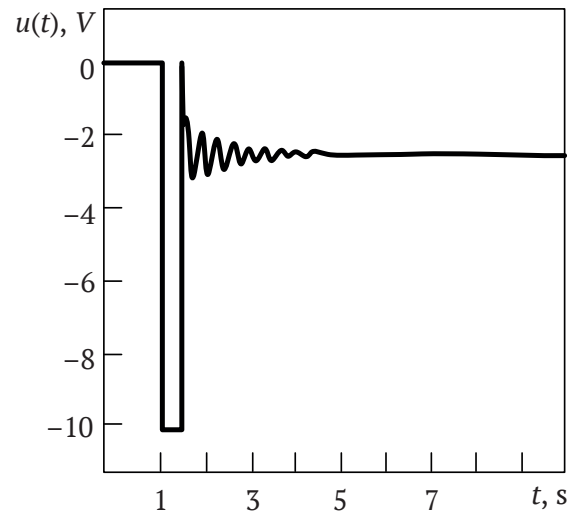


Fig. 13. Type of control action in the course of automatic digging

The simulation results are shown in the form of curves of depth of cut change in the process of automatic digging for the assignments *a*, *b*, respectively. They are presented below in Fig. 12. In addition, Fig. 13 shows a general view of the control action during automatic digging.

The quality indicators of the controllable digging process in rocks with specific resistance $k_p = 1.45 \pm 0.45$ kg/cm² and $k_p = 3.35 \pm 0.75$ kg/cm² are almost identical. Overregulation in the first case is 7.2 %. In the second it is 10.4 %. Control time in the first case is 4 s, in the second, 3.5 s.

Conclusion

The automatic digging operation control system allows the digging trajectory to be practically optimal. It ensures extremely quick penetration of no more

than 3 sec with permissible overregulation of no more than 10%, with following even digging at a constant cut depth. Cut depth is set externally.

The automatic control system lead to decreased loads on the electromechanical equipment and allows for an increase in operational productivity of a walking dragline excavator.

The integrated system of the dragline work process control can be almost autonomous due to the following factors: automatic digging operation control; automatic systems of transporting loaded bucket to the dump and empty bucket to the face; systems of automatic protection against overload of the main mechanisms; and control system for safe movement of the bucket in the dragline working space.

References

1. Ponnusamy M., Maity T. Recent advancements in dragline control systems. *Journal of Mining Science*. 2016;52:160–168. <https://doi.org/10.1134/S106273911601025X>
2. Liu H., Kearney M., Austin K. Development of dragline excavation model for operation planning. In: *Australasian Conference on Robotics and Automation, ACRA*. 2016. Pp. 55–63. URL: <https://www.araa.asn.au/acra/acra2016/papers/pap107s1.pdf>
3. Corke P., Winstanley G., Dunbabin M., Roberts J. Dragline automation: experimental evaluation through productivity trial. In: Yuta S., Asama H., Prassler E., Tsubouchi T., Thrun S. (eds.) *Field and Service Robotics. Springer Tracts in Advanced Robotics*. Springer, Berlin, Heidelberg. 2006;24:459–468. https://doi.org/10.1007/10991459_44
4. Liu H., Kearney M.P., Austin K.J. Dragline operation modelling and task assignment based on mixed-integer linear programming. *Optimization and Engineering*. 2018;19:1005–1036. <https://doi.org/10.1007/s11081-018-9386-5>
5. Htay W.Z., Pevzner L.D., Temkin I.O. Algorithmic and hardware support for on-board information system of walking dragline excavator. *Mining Informational and Analytical Bulletin*. 2019;(2):190–196. <https://doi.org/10.25018/0236-1493-2019-02-0-190-196>
6. Gölbaşı O., Demirel N. Investigation of stress in an earthmover bucket using finite element analysis: A generic model for draglines. *Journal of the Southern African Institute of Mining and Metallurgy*. 2015;115(7):623–628. <https://doi.org/10.17159/2411-9717/2015/v115n7a8>



7. Kumar A., Nandikanti S., Batchu C. Analysis of stress distribution on the bucket of a dragline machine. *Journal of Mines, Metals and Fuels*. 2016;64(5-6):118–122.
8. Ha Q., Santos M., Nguyen Q., Rye D., Durrant-Whyte H. Robotic excavation in construction automation. In: *IEEE Robotics & Automation Magazine*. 2002;9:20–28. <https://doi.org/10.1109/100.993151>
9. Vul Yu. Ya., Kluchev V.I., Sedakov L.V. *Adjustment of electric drives of excavators*. Moscow: Nedra Publ.; 1975. (In Russ.)
10. Pevzner L.D. Automated control system for heavy cyclic excavators. *Russian Mining Industry*. 2011;(5):58. (In Russ.). URL: <https://mining-media.ru/ru/article/karertekh/842-avtomatizirovannaya-sistema-upravleniya-tyazhelymi-ekskavatorami-tsiklicheskogo-dejstviya-2>
11. Pevzner L.D. *Automated control of heavy-duty single-bucket excavators*. Moscow: Gornoe Delo Publ.; 2014 p. (In Russ.)
12. Winstanley G.J., Corke P.I., Roberts J.M. Dragline swing automation. In: *IEEE International Conference on Robotics and Automation*. Albuquerque, New Mexico, USA. 1997;3:1827–1832. <https://doi.org/10.1109/ROBOT.1997.619053>
13. Ridley P., Corke P. Dragline Automation. In: *Proceedings 2001 ICRA. IEEE International Conference on Robotics and Automation (Cat. No.01CH37164)*. Seoul, Korea (South). 2001;4:3742–3747. <https://doi.org/10.1109/ROBOT.2001.933200>

Information about the authors

Leonid D. Pevzner – Dr. Sci. (Eng.), Professor, Institute of Cybernetics, MIREA – Russian Technological University, Moscow, Russian Federation; Scopus ID [37093879700](https://orcid.org/0000-0001-9000-1000); e-mail: lpevzner@msmu.ru

Nikolay A. Kiselev – Undergraduate, Institute of Cybernetics, MIREA – Russian Technological University, Moscow, Russian Federation; e-mail: gost1996@gmail.com

Received	11.07.2021
Revised	17.09.2021
Accepted	01.02.2021